NASA-CR-201493

HUGHES DANBURY OPTICAL SYSTEMS

HUGHES AIRCRAFT

PR C19-0005

FINAL

IN-74-CR

OCIT

63479

PIDDP

FINAL REPORT

PLANETARY HYPERSPECTRAL IMAGER (PHI)

JULY 12, 1996

HUGHES DANBURY OPTICAL SYSTEMS, INC.
100 WOOSTER HEIGHTS ROAD
DANBURY, CT 06810-7589
TELEPHONE (203) 797-5000

Table of Contents

PROJECT SUMMARY

The purpose of the PIDDP contract awarded to HDOS was to demonstrate technology for hyperspectral imaging that would build upon HYDICE, the hyperspectral imager HDOS delivered to NRL. The concept for the space instrument was called PHI, the Planetary Hyperspectral Imager. PHI would be a candidate to replace prior flight instruments such as NIMS and VIMS, providing better signal to noise ratio (SNR) and image quality over the same spectral range for less than half the weight and power.

Two major objectives were proposed to NASA HQ, to be demonstrated with a laboratory breadboard:

1) Extension of the HYDICE spectrometer range, from 400 - 2500 nm (2.5 spectral octaves) to 400 - 5000 nm (3.5 spectral octaves). A single HYDICE focal plane is used to cover the entire spectral range. A sapphire prism is substituted for the glass prism used in the HYDICE design.

2) Substantial reduction of the thermal infrared background. On HYDICE, the thermal infrared background limits performance, decreasing dynamic range and SNR despite instrumental cooling. In extending the spectral range to 5000 nm, the problem is exacerbated. For planetary exploration, the substantial instrumental cooling required to limit this background is not possible for orbits around the terrestrial planets.

A novel background reduction approach was proposed, utilizing a relay to produce a cold stop at a pupil, combined with a spectrometer slit produced on a reflective optic that reimages the cold pupil back upon itself. This design approach was utilized in the breadboard HDOS constructed.

Test data for the infrared background was taken by reading out the focal plane for a hundred frames each of 60 µseconds integration time with the toroidal slit in place. The experiment was repeated with a fold flat substituted in the optical train to view a spectrometer wall instead of the slit. The data were averaged, corrected for offset, and compared.

A net thermal infrared background reduction of between 8 and 10 was achieved. The original objective was to achieve background reduction by a factor of 20.

A spectrum was taken by placing an incandescent source and a polystyrene filter before the spectrometer slit. The spectrum indicates successful spectrometer operation over the spectral range of 450 to 4950 nm, comparable to the 400 nm to 5000 nm spectral range originally proposed.

List of Figures

List of Tables

PIDDP Final Report
July 11, 1996

1.0 PROPOSED OBJECTIVES

The following objectives were proposed for our PIDDP investigation:

1) Assemby of a spectrometer breadboard and testing of that breadboard. We incorporated a HYDICE focal plane and re-imaging optics into a test dewar and aligned them, using a helium neon laser. The HYDICE focal plane was then integrated with laboratory readout electronics. We then assembled and aligned the spectrometer optics and a reflective slit optic, using the helium neon laser. The HYDICE focal plane and laboratory readout electronics were used to measure the background levels associated with the reflective slit optic and a substitution fold flat that allowed the focal plane to view the spectrometer cavity. The ratio of these measurements determines the level of background rejection attained with this novel design enhancement. A background reduction level of 3.8 was measured in Region C, the focal plane portion with the greatest sensitivity. Coupled with an estimated reduction in background from inclusion of the cold stop of 2.2, the overall background was reduced in intensity by a factor of 8. Thus the objective of substantial reduction of the background level with the proposed design was achieved. We also measured a polystyrene spectrum, to demonstrate the spectrometer operation over an extended spectral range stretching from the ultraviolet through the infrared. Again this objective was achieved.

2) Consultation with our Science Advisory Committee (SAC) to structure program efforts to meet near term Solar System Exploration Division (SSED) mission objectives. These consultations led to our Rosetta Orbiter instrument proposal for a Cometary Hyperspectral Imager (CHI) and a response to a Johns Hopkins Applied Physics Laboratory (APL) Request for Information (RFI) for a hyperspectral imager for their Discovery Mission CONTOUR (Comet Nucleus Rendezvous Tour). The CHI proposal and CONTOUR RFI response referenced our PIDDP work. We therefore believe these consultations were successful and this objective was achieved.

3) Focal plane consultations with Santa Barbara Research Center (SBRC) and the science team to ascertain the utility of existing InSb

focal planes for SSED missions and to determine the feasibility of future focal plane enhancements with regard to risk and cost, such as larger array sizes, smaller pixel sizes, lower power dissipation, and improved offset and gain stability. The results of these consultations are tabulated in this final report and therefore were successfully achieved.

2.0 REQUIREMENTS DEFINITION

The requirements for the breadboard design were chosen as

- Spectral Range from $\lambda \leq 400$ nm to $\lambda \geq 5000$ nm within a single spectrometer arm;
- Compact design for low volume and weight;
- Excellent image quality/optical performance;
- Design for decreased background, consistent with cryo-radiator peformance for terrestrial planet observations.

3.0 IMPLEMENTATION AND TRADE-OFFS

Design for decreased backgound is extremely important. For a prism spectrometer with a multi-octave spectral range (HYDICE type design), the focal plane has a large view factor to the spectrometer cavity, resulting in a large offset from thermal background. For the case of an orbit around a comet or asteroid, thermal loading from the asteroid or comet tends to be minimal, due to the small size of the body relative to the size of the orbit or proximity of the flyby trajectory. Consequently for reasonably sized radiators and favorable spacecraft geometry, very cold temperatures ($\leq$ 170K) can be realized for the instrument, substantially reducing the offset from instrumental thermal background. For orbits about Jovian type gas giants (or their moons), thermal loading from the gas giant is high due to the huge size of the planetary limb relative to the orbit. But the thermal loading from the sun is low, due to a distance $\geq$ 5.2 AU, and the gas giant temperature is $\leq$ 170K. Consequently low instrumental temperatures could be realized in these cases as well. However, for the inner planets, it is doubtful that instrument temperatures can be attained in low orbits much colder than the apparent temperature of the planet itself. For example, Mars has an apparent temperature of 224.3K; our thermal model run during the PIDDP proposal indicated the instrument could be cooled to 220K. The situation becomes worse as we get closer to the sun, as planetary apparent temperatures become warmer. Another way to look at the problem is thermodynamically; the relatively large instrument, with a large view factor to the planetary limb, will naturally want to come into radiative thermal equilibrium with that planet (the same holds for the spacecraft surfaces). Generally there will be a large differential between how cold the small focal plane can be run versus the much larger instrument.

The solution proposed in our original PIDDP baseline was to configure the slit as a reflective optical surface, and to reimage the pupil through a cryogenic surface ("cold stop"). The focal plane field of view would then be restricted to the optics, with its relatively low emissivity and small solid angle, as opposed to the view of the spectrometer cavity, which is much larger and has emissivity $\approx$ 1.

Two trade-offs occurred in the implementation of the proposed solution. The first occurred in the implementation of the slit. We could either emulate HYDICE and make a microlithographic slit on a thinned plate of silicon, or develop it on the surface of a field lens. The second trade-off concerned the cold stop, which could be implemented in a refractive lens assembly or reflectively with mirrors.

The slit implementation choice was made on the basis of feasibility and associated risk. The HYDICE slit entailed thinning the silicon slit plate thickness to $\approx$ 3 µm, necessitated by the high speed (f#=3) of the HYDICE system. Because of HYDICE's (or PHI's) high speed, the slit must be extremely thin to avoid vignetting from the small depth of focus. Such extreme thinning was determined to be very difficult to implement on a torroidal surface. For HYDICE the microlithographical slit was produced via a contact method. Again, it was determined this method would not work with a torroidal surface.

Producing a field lens with the necessary surfaces was determined to be relatively simple. The slit could be produced on a lens surface with an appropriate thin metallic coating that would meet requirements for dimensional accuracy, depth, opacity (from the foreoptics side), and low emissivity (from the spectrometer side). The drawback, common to all field lenses, is the potential for surface imperfections being reimaged upon the focal plane, and the potential for stray light from ghosts generated by internal reflections.

For the refractive versus reflective solutions to produce the cold stop, the reflective solution was chosen. A number of factors mitigated against a refractive solution;

1) The number of refractive materials available to cover a large spectral range was extremely limited; the dispersion associated with the large spectral range with available materials resulted in aberrations that could not be corrected and that degraded MTF to unacceptable levels;

2) Stray light would result from the additional refractive surfaces; with a symmetric four lens system that seemed to be the minimum workable solution, there were 28 ghosts (eight refractive surfaces in combination of two at a time) with a ghost level of ≈ 0.1% per ghost (≈ 3% average reflectivity per surface over the spectral range after anti-reflection coating). The total stray light level from ghosts would be ≈ 2.8%. This is five times the stray light level from ghosts for HYDICE, and would double the stray light level (≈ 3%) achieved for HYDICE, where the dominant stray light came from tolerances on the reflective optics and diffraction.

3) Throughput losses from the anti-reflection coating inefficiency would be ≈ 22%.

4) The lens system is sensitive to misalignments such as tilts, decenters, and despace.

The alternative solution would be a reflective solution. This approach has the inherent advantage of working over a large spectral range, with minor impact on stray light levels.

The specific reflective solution found is shown in Figure 1. It is a ring field solution, implemented in semiconductor micolithographic mask production equipment. The two mirrors are both spheres, with the cold pupil located on the small sphere. A total of three reflections are required in this solution. Additionally a refractive field lens is required near the location of the focal plane of the Schmidt spectrometer. This mirror system is relatively insensitive to misalignment; the greatest sensitivity is to despace between the

FIGURE1 - REFLECTIVE SOLUTION TO GENERATE COLD STOP

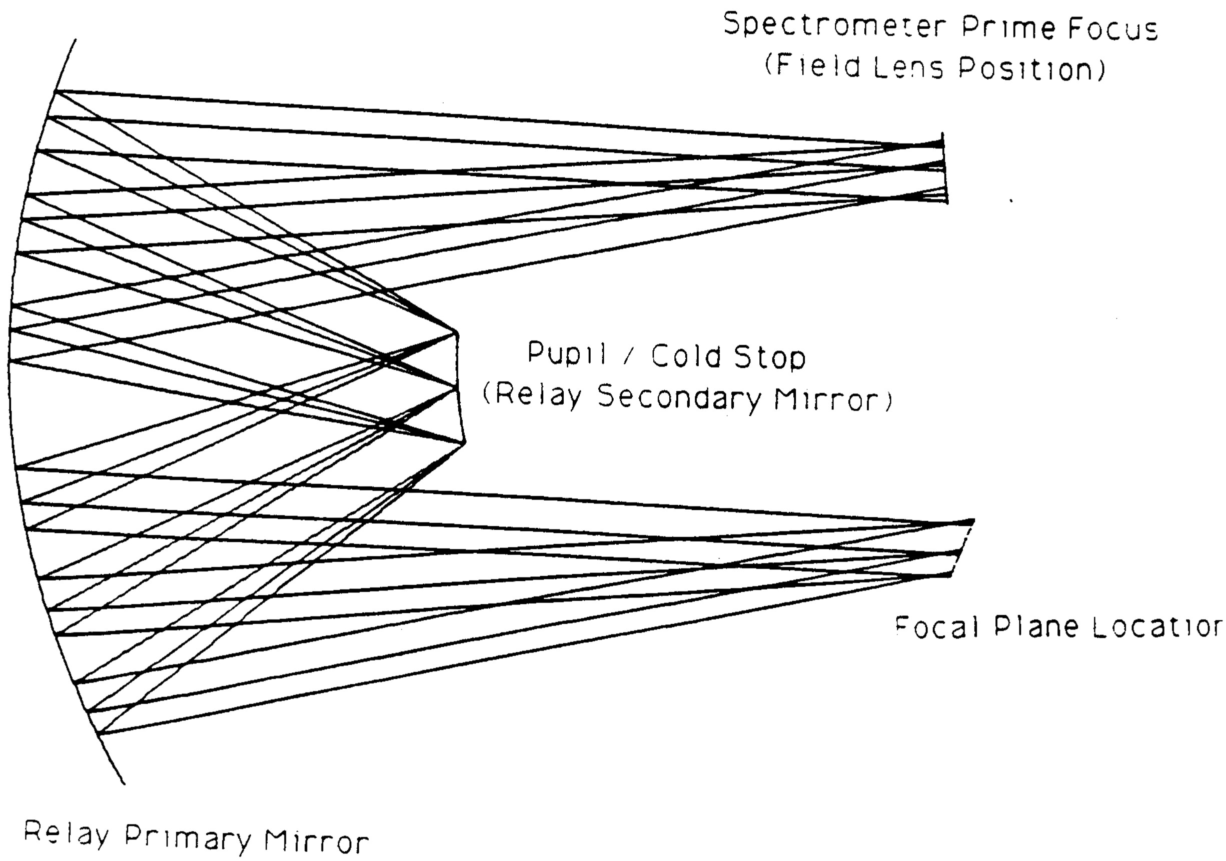

primary and secondary. The major drawback are the three reflections in the ultraviolet. Using aluminum with magnesium flouride overcoats for the mirrors, the net loss in throughput at 300 nm of 33%. For the well known minimum in reflectivity of aluminum at 850 nm, the loss in throughput is 39%. Using enhanced silver coatings, the three reflections would produce a throughput loss ≤ 10% in the visible and infrared, but the ultraviolet would be lost. The weight for implementation would be ≈ 1 lb.

A major trade-off also occurs in selection of a prism material. It is highly advantageous to choose a high dispersion material to mininimize instrument size and weight. The greater the angular dispersion the prism can supply, the shorter the instrument can be to achieve the required linear dispersion, decreasing size and weight. Going to a larger prism apex angle generally does not help decrease instrument weight. The weight savings due to decreased instrument length is offset by the increase in the weight of the prism due to its larger base; the prism can be the dominant weight element of the instrument. The dispersion of a set of prism materials is graphed in Figure 2a and 2b. The dispersions of magnesium flouride and calcium flouride are close together; barium flouride has somewhat higer dispersion than either MgF_2 or CaF_2 in the visible, and less dispersion in the infrared. However sapphire and cubic zirconia have much higher dispersions (factors of 3 to 4, depending on the spectral region) than any of the flouride crystals. Compared with each other, cubic zirconia has much higher dispersion in the visible than sapphire (factors of 4 to 10), comparable dispersion to sapphire in the near infrared from 1500 nm to 2500 nm, and lower dispersions in the infrared (factors of 1.5 to 2). The more uniform dispersion of sapphire, its larger spectral range (cubic zirconia's transmission is confined to the spectral region 400 nm to 5000 nm), its higher dispersion in the infrared which is useful for identifying mineral absorptions, led us to baseline this material for the PIDDP prism. The expected spectral resolution $\lambda/\Delta\lambda$ of a sapphire prism coupled to our HYDICE focal plane is shown in Figure 3 for the spectral range 300 nm to 5000 nm.

The breadboard concept of Figure 4 was designed to test the concept. To fit the focal plane and reflective relay optics into an available dewar, some folding of the beam was necessary, as shown in Figure 4. The optical performance of the breadboard design is excellent, as shown by the spot diagram of Figure 5. For the cold optics within the dewar, the optical material was chosen to be pyrex (Ohara E-6 low

FIGURE 2A - DISPERSION OF PRISM MATERIAL CANDIDATES, ULTRAVIOLET THROUGH INFRARED

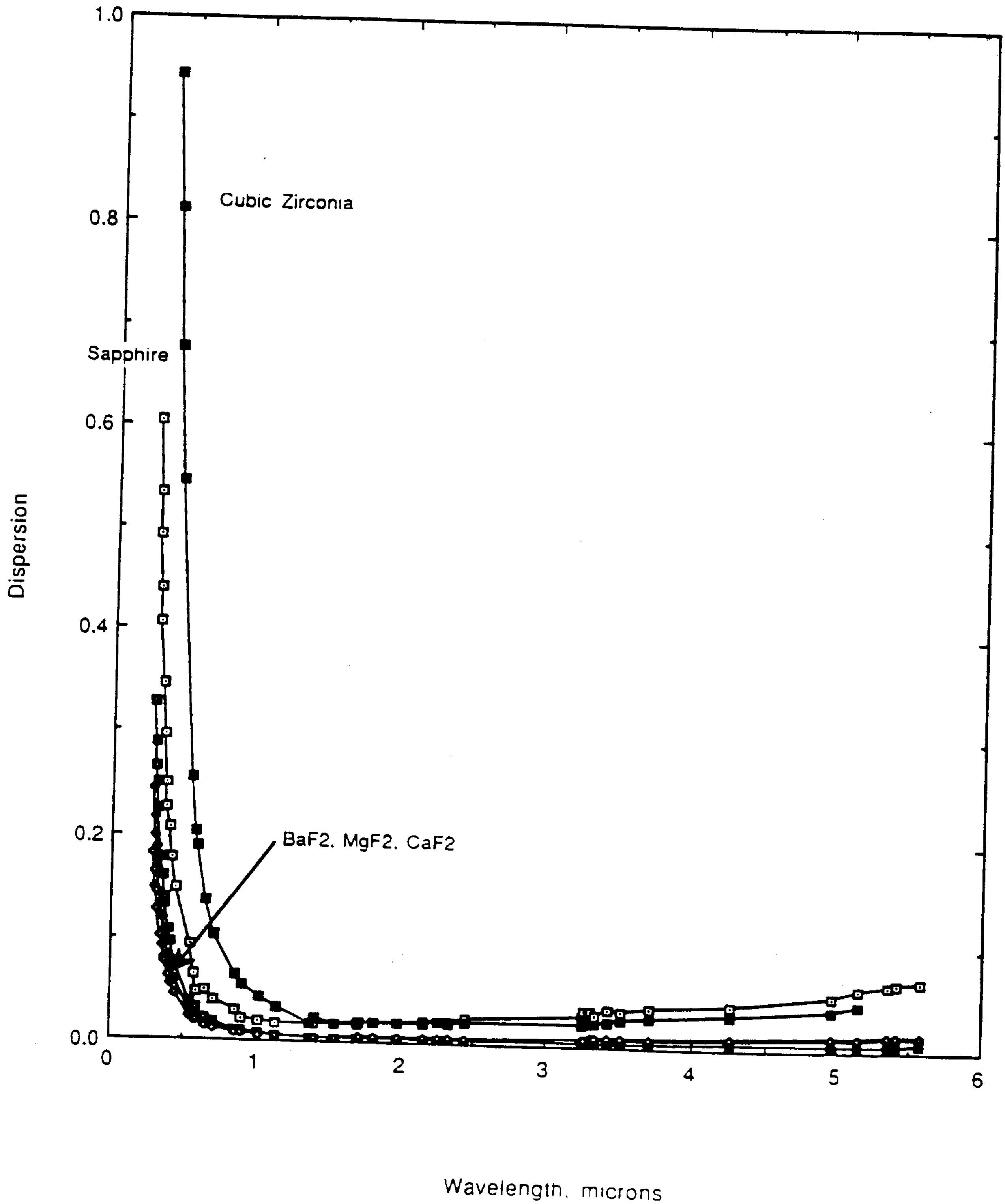

FIGURE 2B - DISPERSION OF PRISM MATERIAL CANDIDATES, VISIBLE THROUGH INFRARED

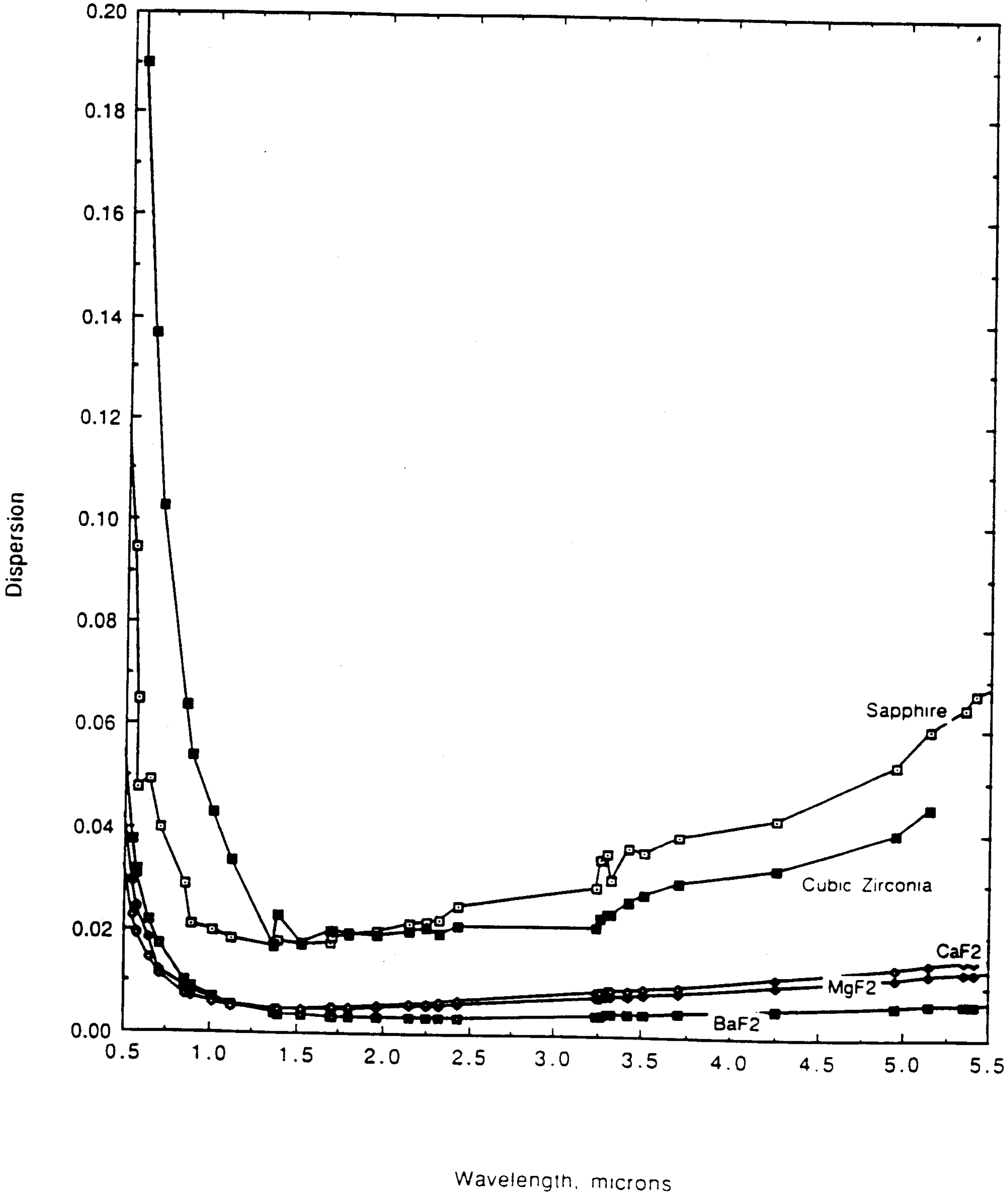

FIGURE 3 - SPECTRAL RESOLUTION FOR PIDDP BREADBOARD

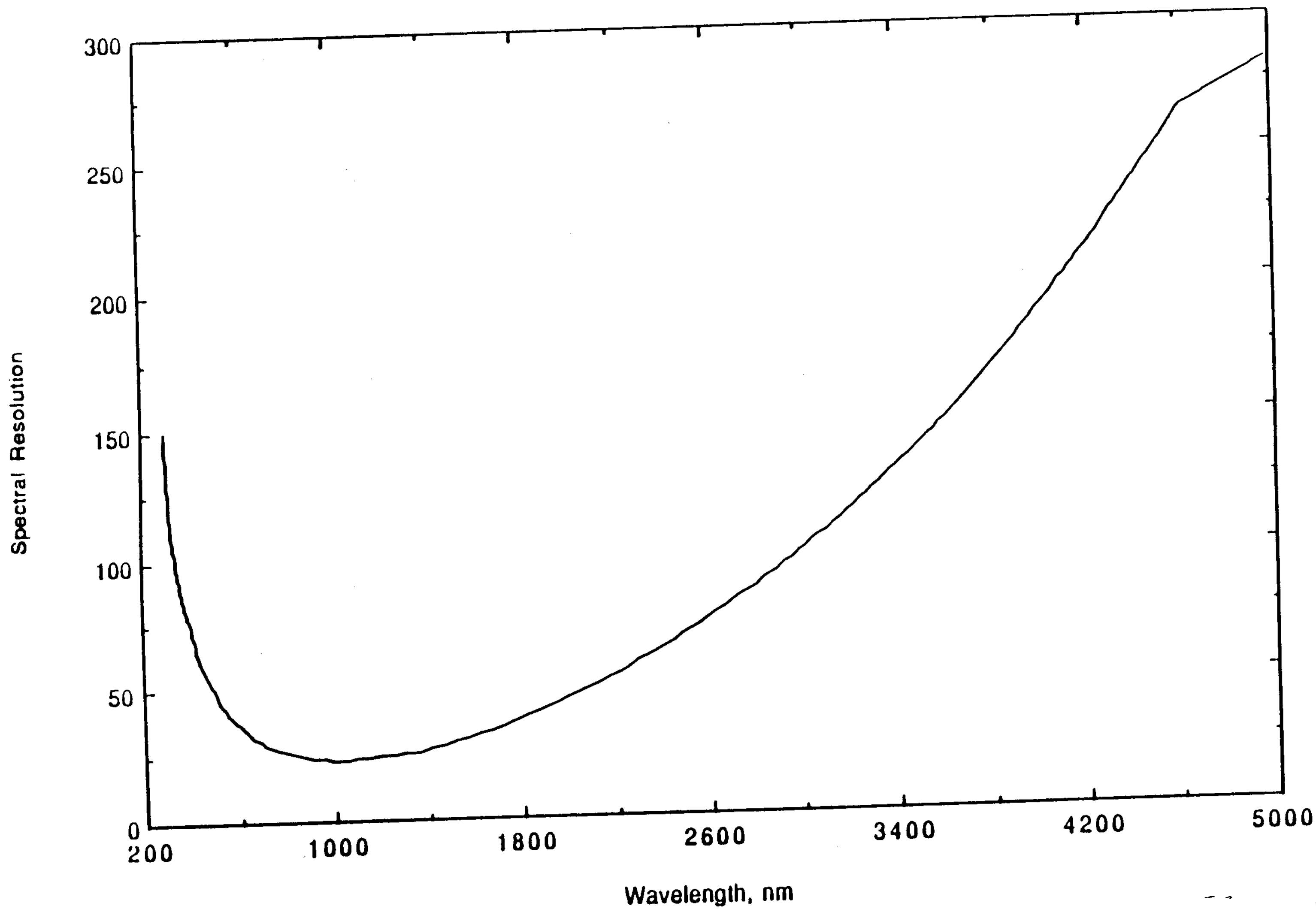

FIGURE 4 PIDDP BREADBOARD CONCEPT

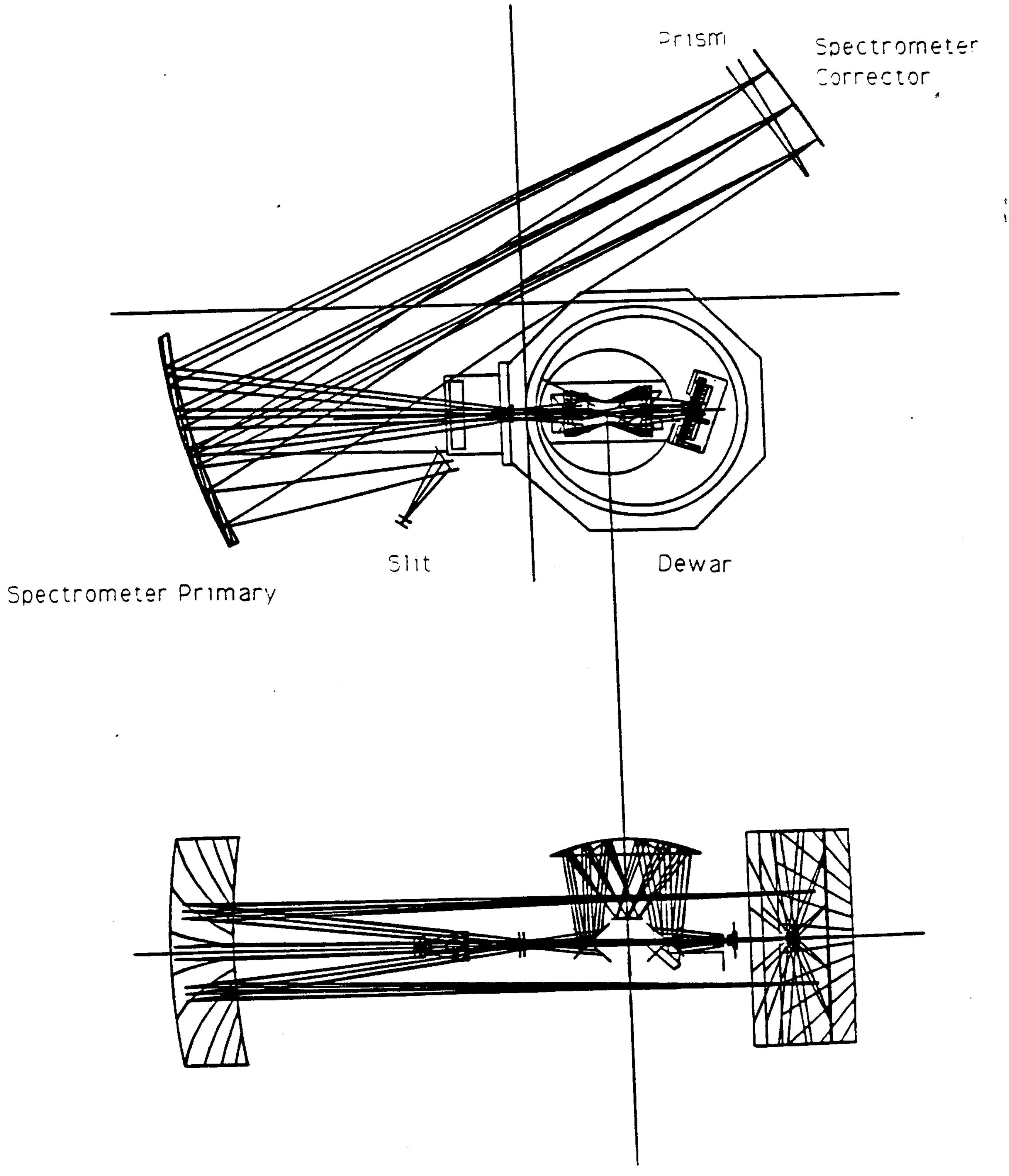

FIGURE 5 - SPOT DIAGRAM FOR PIDDP BREADBOARD SPECTROMETER WITH REFLECTIVE RELAY

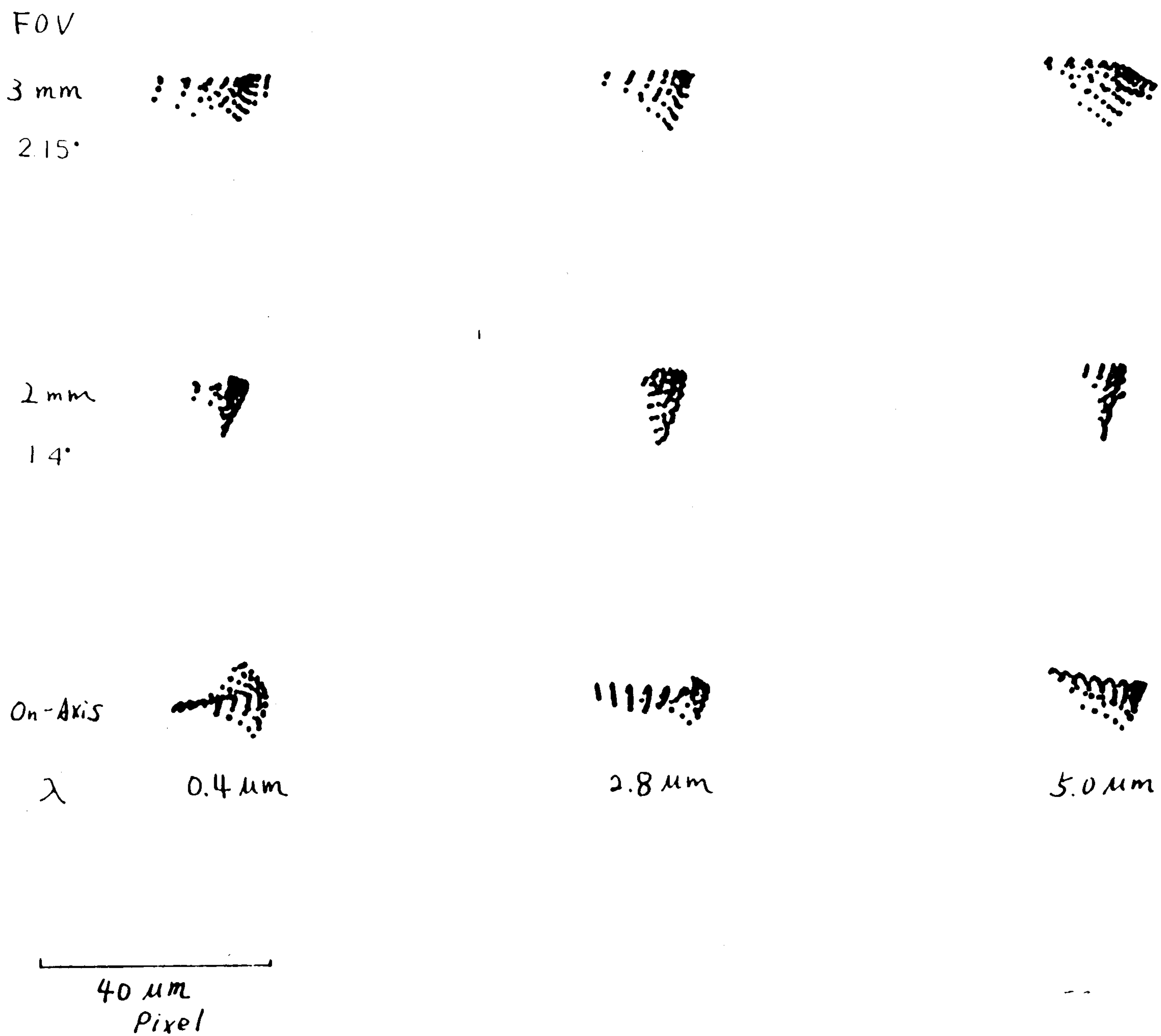

expansion glass), while the mounting material was chosen to be invar because of the extremely good CTE match between the materials to LN2 temperatures (Figure 6). The cold invar mounting cylinder provides excellent stray light control. It was decided to coat the sides of the prism with an anti-reflection coating, since the effective emissivity of the prism would be ≈ 12% otherwise, and could mask the effective background reduction we expect to demonstrate.

4.0 FOCAL PLANE CONSIDERATIONS

At the Division of Planetary Sciences (DPS) meeting (October, 1996), I met with Drs. James Bell and Roger Clark. While they were generally supportive of the PIDDP effort and goals, a desire for increased spectral resolution was expressed. Dr. Clark believed that an increase in spectral resolution of the baseline PIDDP by a factor of two would yield a much improved science return. Important spectral bands that would be barely resolved with the baseline PIDDP would be adequately resolved and sampled with a resolution improvement of a factor of two. Table 1 (Courtesy of Dr. Bell), a compilation of important spectral bands for ice recognition, is of value for comets and for planetary gas giant moons. It provides an illustration of this consideration. According to Dr. Clark, when at least two spectral resolution elements covers the FWHM of a species, the SNR required to detect that species is much reduced. This more than compensates for the halving of the signal incident on each spectral pixel due to spreading the available signal over two pixels rather than a single pixel. Thus 400 spectral pixels would be desired, in contrast to the 210 pixels currently available with the HYDICE focal plane. Table 1 indicates the higher spectral resolution focal plane would provide four times the science return of the PIDDP focal plane.

As part of our PIDDP proposal we stated we would ascertain the utility of existing InSb focal planes for SSED missions. Table 2 summarizes the existing state of the art of existing SBRC InSb focal planes that could be relevant to the hyperspectral application. The first three focal planes were developed for low background, astronomical observations. As such they are low well depth (≈ 200,000 electrons), but have low noise, achieved in part by relatively slow readout rates. Their worst fundamental limitation is their low dynamic range. An observation of a solar type spectrum in reflection over a PIDDP type spectral range (300 nm - 5000 nm)

FIGURE 6 - THERMAL MATCH OF MIRROR AND MOUNTING MATERIALS

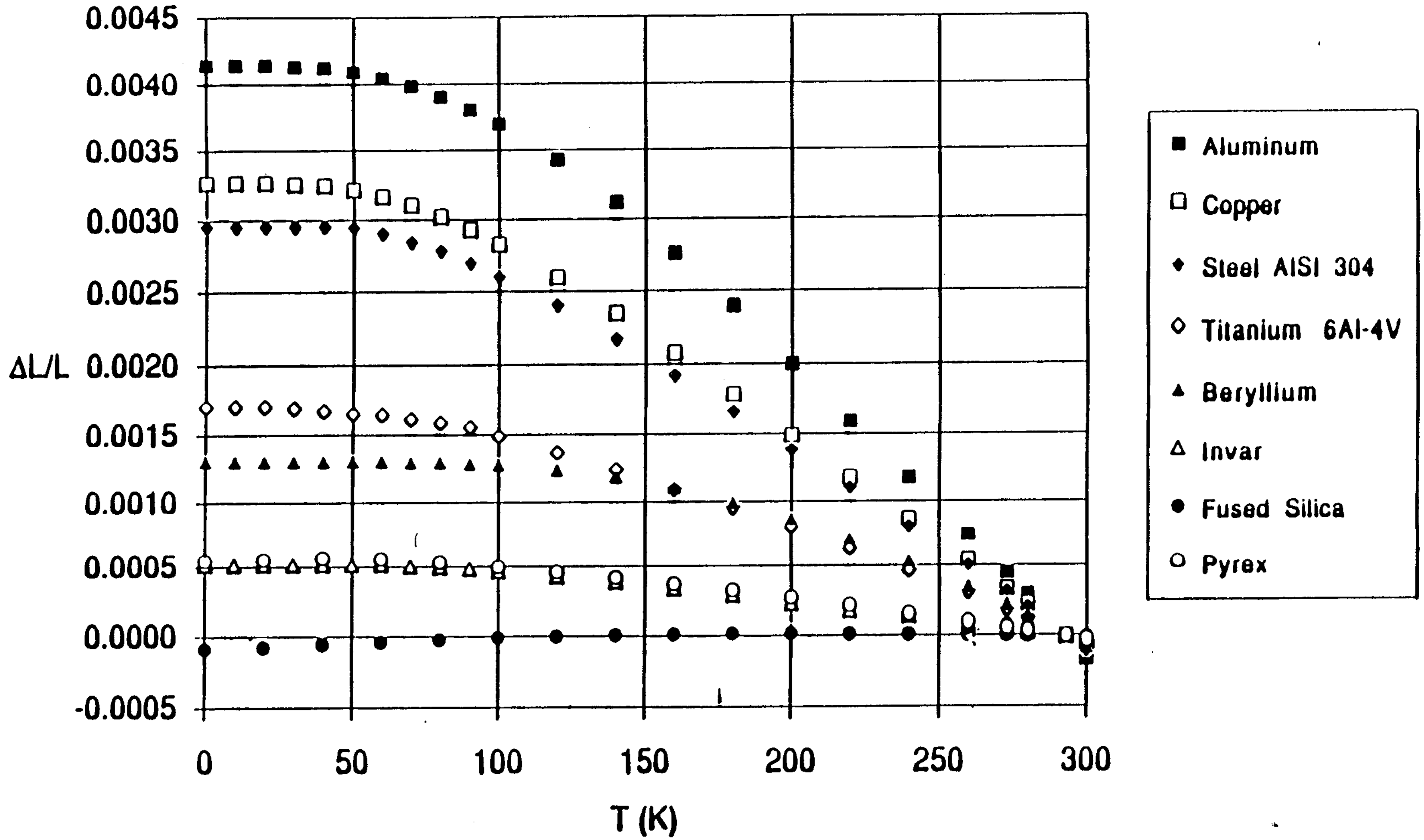

Table 1 Characteristic Vibrational Bands for Potential Ices and Organics - Doubling the Baseline PIDDP Resolution Vastly Improves the Capability for Material Identification

Species	Band Center (nm)	FWHM (nm)	PIDDP Resolution (nm)	PIDDP Adequacy	Doubled Resolution (nm)	Doubled Res Adequacy
^{12}CO	4672	24	18		9	Y
	2360	8	39		20	
^{13}CO	4785	20	18		9	Y
X(CN)	4619	50	18	Y	9	Y
C-D Stretch	4350 - 4650	60	18	Y	9	Y
$^{12}CO_2$	4274	60	20	Y	10	Y
	2070	6	44		22	
	2010	6	45		23	
$^{13}CO_2$	4386	17	19		10	Y
N_2	4296	5	19		10	
	2147	23	42		21	
HCOOH	3344	25	26		13	Y
Formaldehyde	3466					
	3540					
POM	3380	29	26		13	Y
Polyoxymethylene	3430	35	26		13	Y
	3590	32	26		13	Y
HMT	3390	23	26		13	Y
Hexamethylene-	3420	23	26		13	Y
tetramine	3480	24	26		13	Y
Methanol	2540	18	25		12	
	2273	41	40		20	Y
Microdiamonds	3472	90	25	Y	12	Y

Species	Band Center (nm)	FWHM (nm)	PIDDP Resolution (nm)	PIDDP Adequacy	Doubled Resolution (nm)	Doubled Res Adequacy
Aliphatics	3384	22	26		13	Y
Aromatics	3279	22	26		13	Y
O-H Stretch	3100	280	29	Y	15	Y
Dangling OH	2714	11	33		17	
N-H Stretch	2963	40	31		16	Y
H_2	2416	6	38		19	
CH_4	2370	14	38		19	
	2320	32	39		19	Y
	2200	17	41		20	

Table 2 - Candidate InSb Focal Planes

Focal Plane	Well Depth(s) (electrons)	Noise(s) (electrons)	Size (pixels)	Int. Time (msec)	Dynamic Range	Outputs
Astronomy	200,000	50	256 x 256	≥ 50	4000	1
Aladdin Quadrant	200,000	25	512 x 512	≥ 50	8000	8
Aladdin	200,000	25	512 x 512	≥ 50	8000	32
TV Format	5,600,000	1200	640 X 480	≥ 9	4700	2
HYDICE (PIDDP)	11,000,000 6,600,000 2,200,000	1100 670 270	320 X 210	≥ 9	41000	2
S-092	2,000,000 900,000 200,000	120 90 60	320 X 210	≥ 1	33000	16

requires a dynamic range in excess of 40000. Otherwise when allowing the spectral distribution at the solar peak in the visible to reach maximum well depth at maximum reflectance, the signal in the ultraviolet may be only several tenths of a percent of the well depth ($\approx$ 600 photoelectrons), producing a SNR of $\approx$ 10. Alternatively if we integrate for a long time period to get adequate SNR in the ultraviolet, we would saturate the focal plane in the visible portion of the spectrum. Other important limitations are the relatively long times to read out the array which may be excessive for flybys or orbits about terrestrial planets, and the large number of outputs associated with the newest astronomy arrays, which imply multiple electronics boards that would be inconsistent with Discovery mission goals for power and weight. The fourth entry is a focal plane that was designed for high signal applications in an interlaced format. Its major attribute is its large number of pixels. Again, its dynamic range is inadequate for hyperspectral applications.

The HYDICE focal plane, designed as it was for earth remote sensing hyperspectral applications, has adequate dynamic range. However, as pointed out above, its spectral resolution does not provide optimal science. Moreover, because of its earth remote sensing origin, its well depth and resulting noise is excessive in the ultraviolet. For the earth, Rayleigh scattering from the atmosphere produces an effective albedo of $\geq$ 50%, where as the reflected ultraviolet from a body with no atmosphere might only be several per cent. The S-092 chip is a low well depth / low noise version of the segmented HYDICE focal plane, using CTIAs (charge transfer impedance amplifiers). It is suitable for short integration times that would be associated with high spatial resolution mapping from earth orbit or for mechanical scanning. Like the HYDICE array, its spectral resolution does not provide optimal science, nor does it provide adequate SNR in the ultraviolet. Moreover, its large number of outputs implies multiple electronics boards that would be inconsistent with Discovery mission goals for power and weight. The CTIAs also dissipate much more power than the direct injection amplifiers of the HYDICE focal plane. The power dissipation is incompatible with passive cryoradiators. This is a problem for Discovery type missions where mechanical cryocoolers capable of handling the higher power dissipation would have excessive weight and power.

Expansion of the HYDICE focal plane to 400 spectral rows, with an additional fourth segment for the ultraviolet, has been discussed with Dr. Alan Hoffman of SBRC. Dr. Hoffman is the Program Manager for SBRC astronomical focal plane arrays and an expert on InSb focal planes. The fourth segment is not seen as having any significant impact on the multiplexer yields. The 400 spectral rows are compatible with the field size of the Ultratech Stepper used to produce the multiplexer. Because focal plane power dissipation is overwhelmingly (95%) dominated by the readout rate through the output amplifiers for the direct injection focal plane, the doubling of the number of spectral rows will not affect the ability to cool the focal plane with a passive cryoradiator.

In conclusion, a focal plane with twice as many spectral rows with a region optimized for ultraviolet spectral imaging is feasible. I would recommend NASA consider sponsoring the development of such a focal plane.

5.0 BREADBOARD ASSEMBLY AND RESULTS

The integration of the optics into the breadboard assembly began with the dewar optics. In Figure 7, we show the invar assembly with the two fold flats and relay secondary mirror in place. The incident ray bundle enters the assembly through a hole in the invar shell on the right and is reflected off a fold flat to the relay primary mirror (not shown) at the top of the assembly. The primary mirror reflects the light to the relay secondary mirror (center), a pupil that acts as the optical system's cold stop. The secondary then reflects the light upwards once again to the relay primary. The relay primary then reflects the light to the fold flat (left) and out the hole in the invar shell on the left to the focal plane assembly, where it comes to a focus on the InSb focal plane.

The relay primary mirror was then assembled into its position at the top of the invar assembly. In Figure 8 we show the invar assembly in its position on top of the dewar cold plate, next to the dewar outer shell. Note the sapphire window in the dewar outer shell, through which light enters the invar dewar assembly (through the hole in the left of the assembly as shown in this picture). When the dewar outer shell is in place, the dewar assembly is inverted and liquid nitrogen brings the entire invar assembly, including the InSb focal plane, to its operating temperature of 80K.

Figure 7

Internal View of Invar Assembly with Optics In Place

HUGHES AIRCRAFT

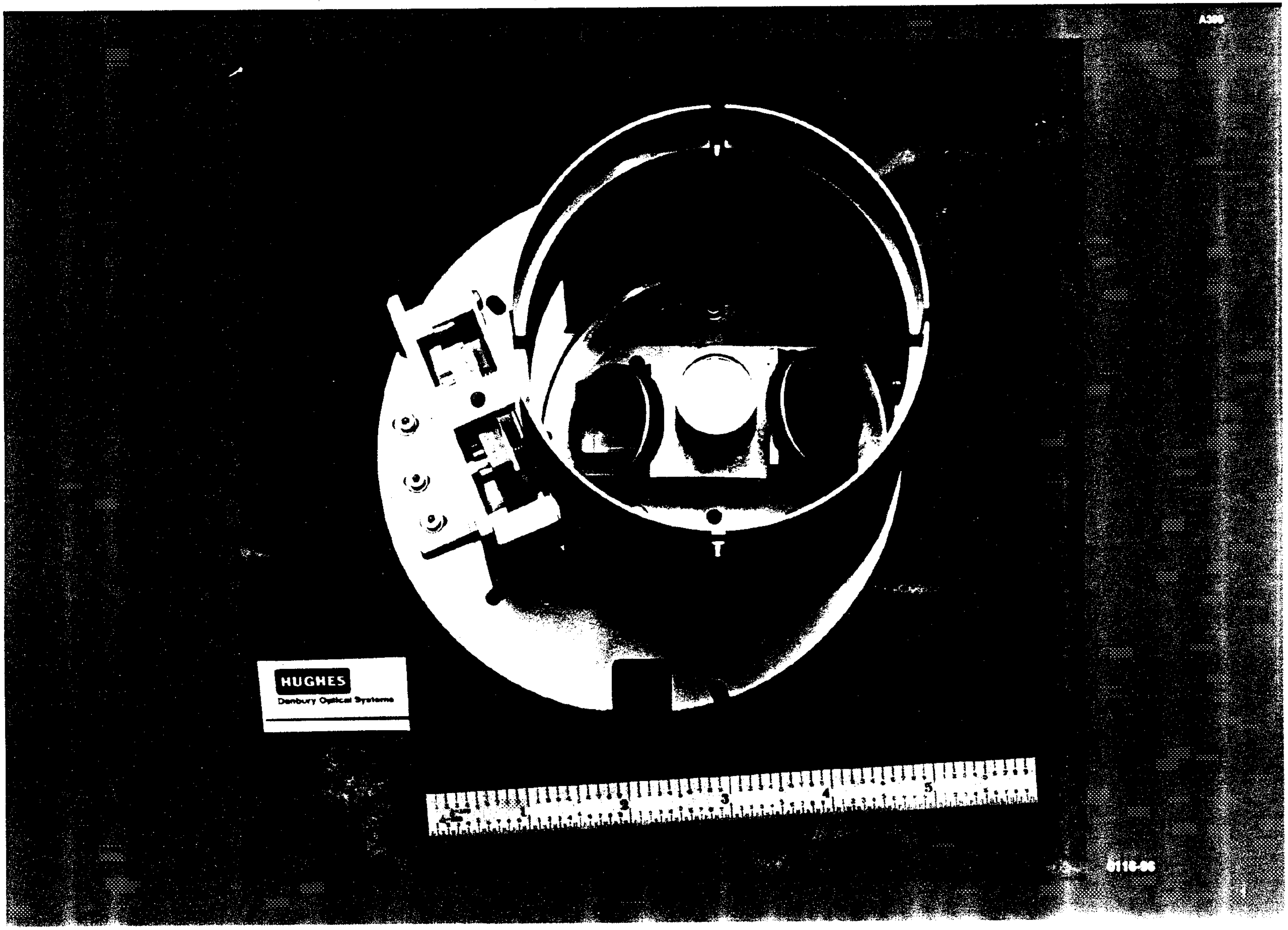

The focal plane assembly is at the left. The secondary mirror, where the cold stop is located, is in the assembly center, with fold flats needed for the compact packaging on either side.

Figure 8

HUGHES
AIRCRAFT

PIDDP Dewar Assembly

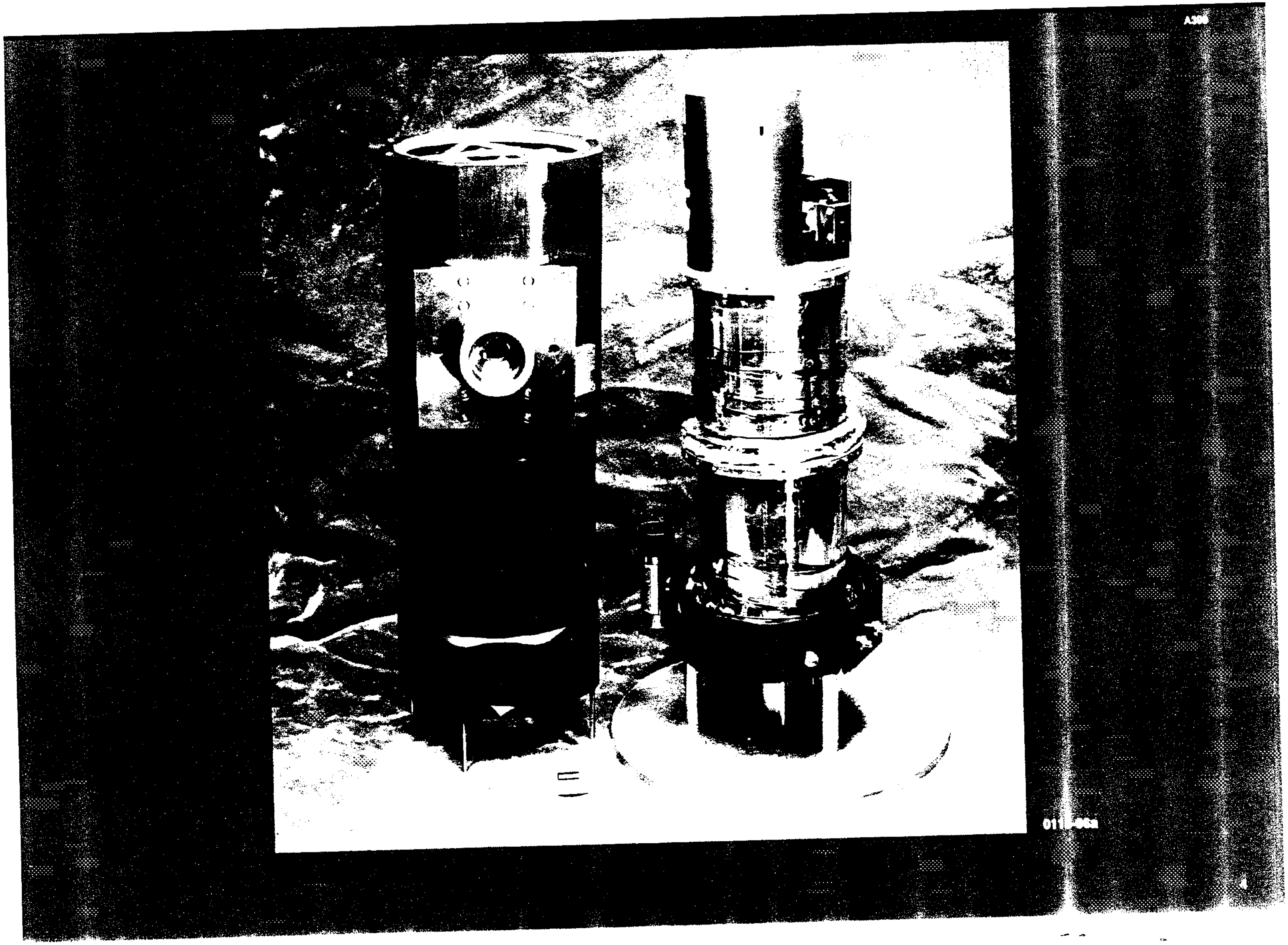

The prism was anti-reflection coated with magnesium fluoride. As noted earlier it was judged important to do this to keep the overall background at a low level. A theoretical coating model indicated an average throughput for the prism in a single pass of 0.92 could be realized (Figure 9); the fall off toward 5 μm is due to internal absorption by the sapphire. An uncoated prism would have losses of ≥12% in single pass due to Fresnel reflection, and indeed losses of 15% were measured on the uncoated witness sample (Figure 10). The science team had expressed some skepticism as to whether the prism anti-reflection coating could in fact provide this level of transmission over the 3.5 octaves of spectral range. Measurements (Figure 11a) of the coated witness sample indicates that performance in the visible was better than the model prediction; performance in the infrared (Figure 11b) was in general agreement with the model, but was somewhat worse in some spectral regions. Around 2.9 μm the throughput is ≈ 5% lower than predictions in an interference ripple; beyond 4.4 μm the spectral transmission declined faster than predicted, due apparently to greater internal absorption by the sapphire than had been predicted.

A preliminary alignment of the prism into the spectrometer was performed to verify the system did indeed work as a spectrometer. The focal plane was taken down to temperature to verify that it was optically active and that signals from the focal plane could be processed with the Amber test station. The toroidal slit (Figure 12) was incorporated into the spectrometer. A helium-neon laser (633 nm) was used to complete the spectrometer alignment, placing the beam onto row 29 of the focal plane. The breadboard alignment was found to be sensistive to relative motions of the spectrometer corrector and the dewar. Corrector motions produced astigmatism, spreading the beam in the spatial direction. Motions of the dewar produced defocus and a symmetric spreading of the beam. Alignment was completed to focus the laser to a spot, completing the breadboard (Figure 13).

The thermal infrared background was measured as described in section 1.6.2.4 of our original PIDDP proposal. The spectrometer background was integrated for 60 μseconds and the focal plane voltages were readout. This was done for a hundred frames and the voltages from the different frames were averaged. A fold flat was then inserted in front of the toroidal slit so that the spectrometer wall was viewed in stead of the slit. The background was then integrated for 60 μseconds. This was done for a hundred frames and

Figure 9

Sapphire Prism Throughput, Coating Model

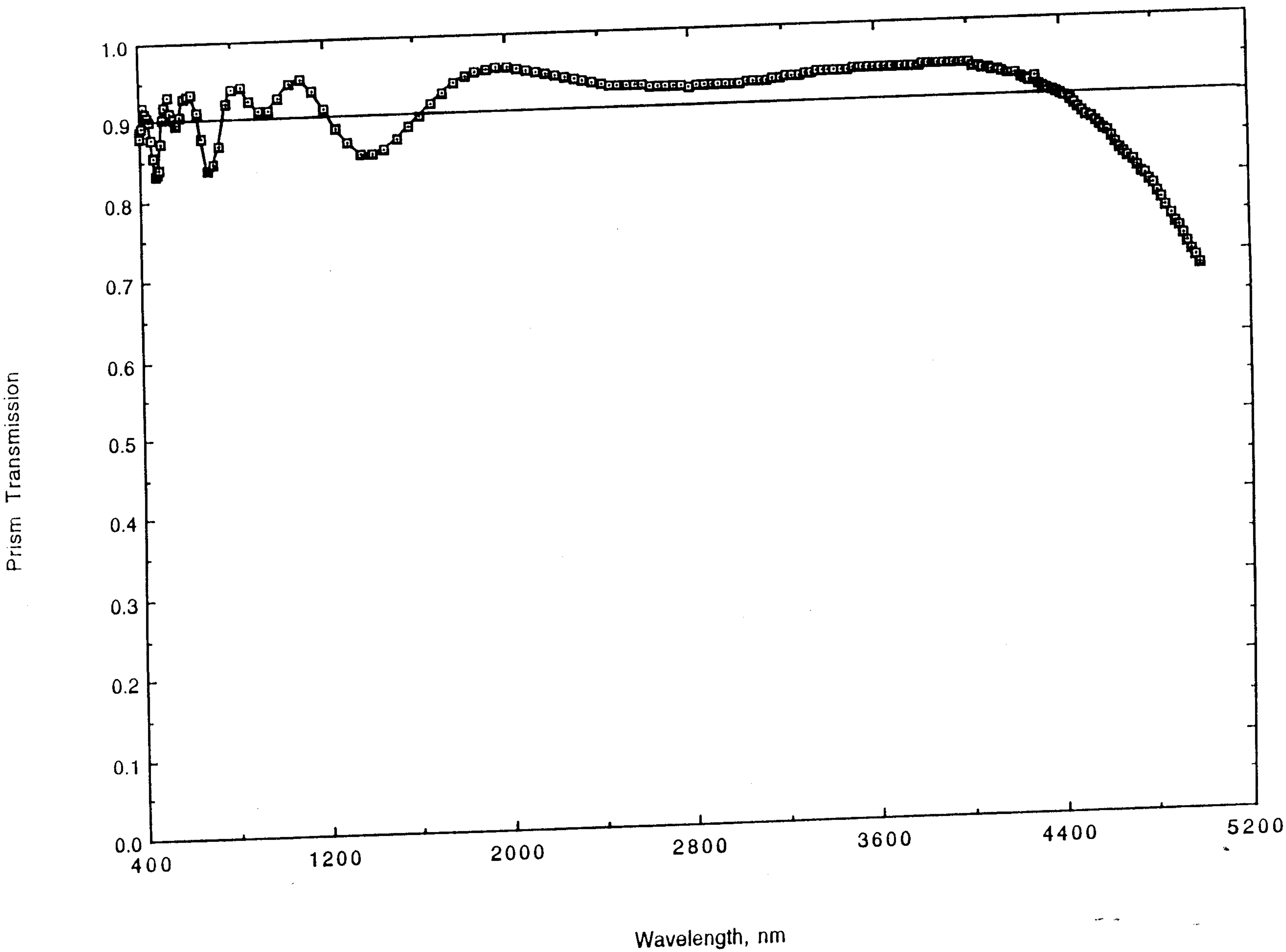

uncoated witness piece

3/20/96 HB

Figure 10 Throughput of Uncoated Sapphire Witness Sample

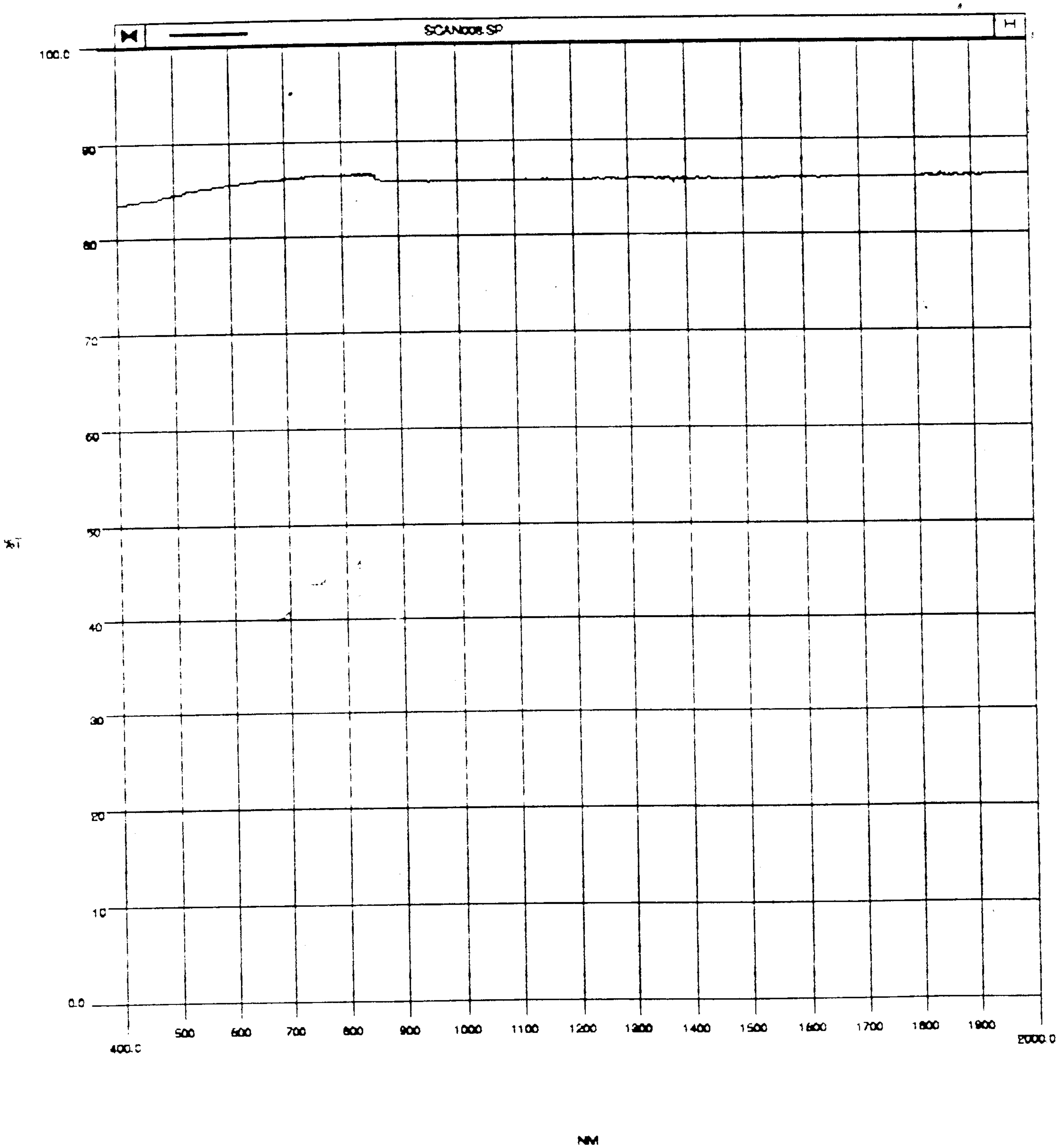

R1 & R2 COATED
3/21/96

Figure 11a Throughput of Coated Sapphire Witness Sample, Visible Through SWIR

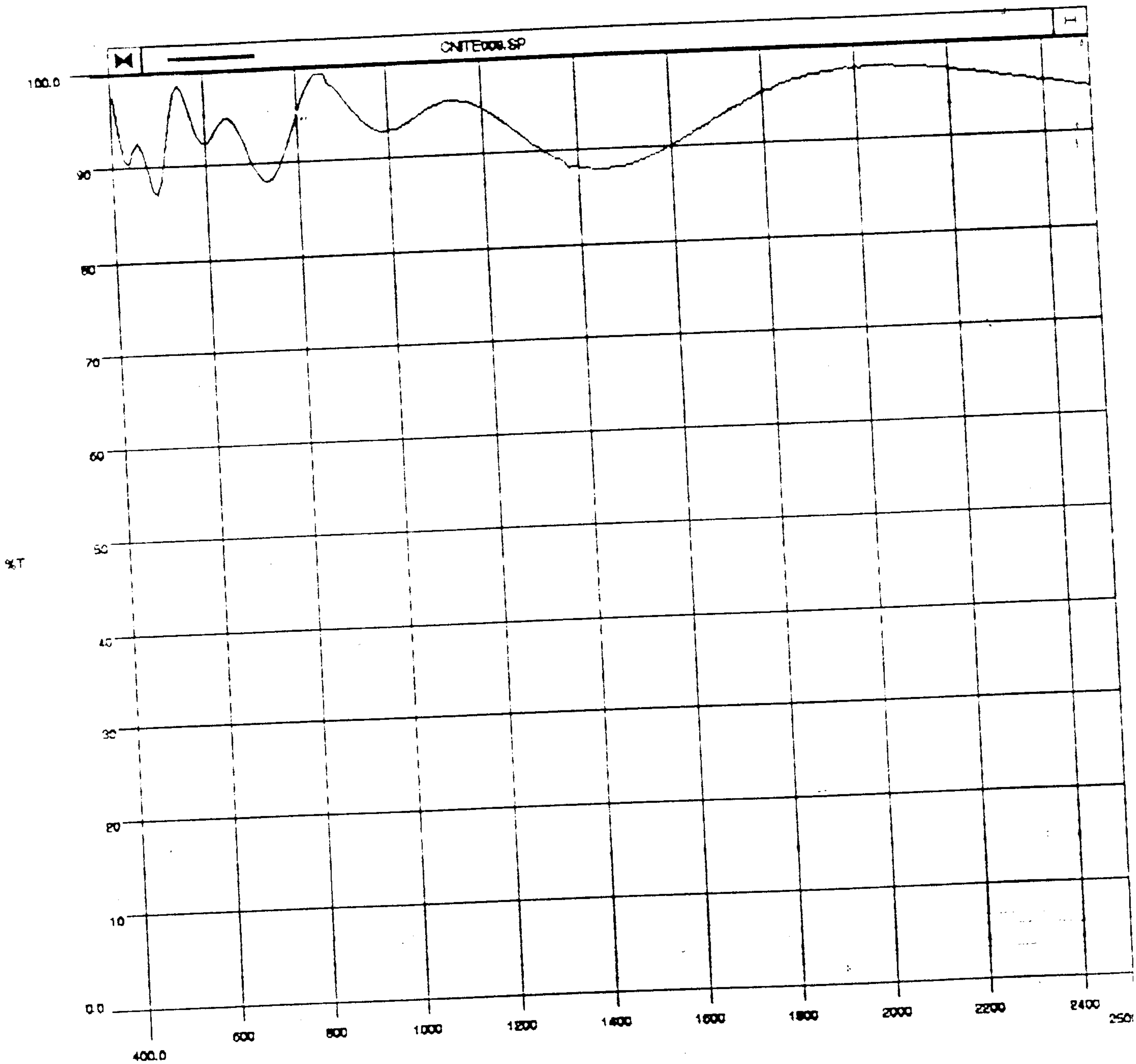

Figure 11b   Throughput of Coated Sapphire Witness Sample, Infrared

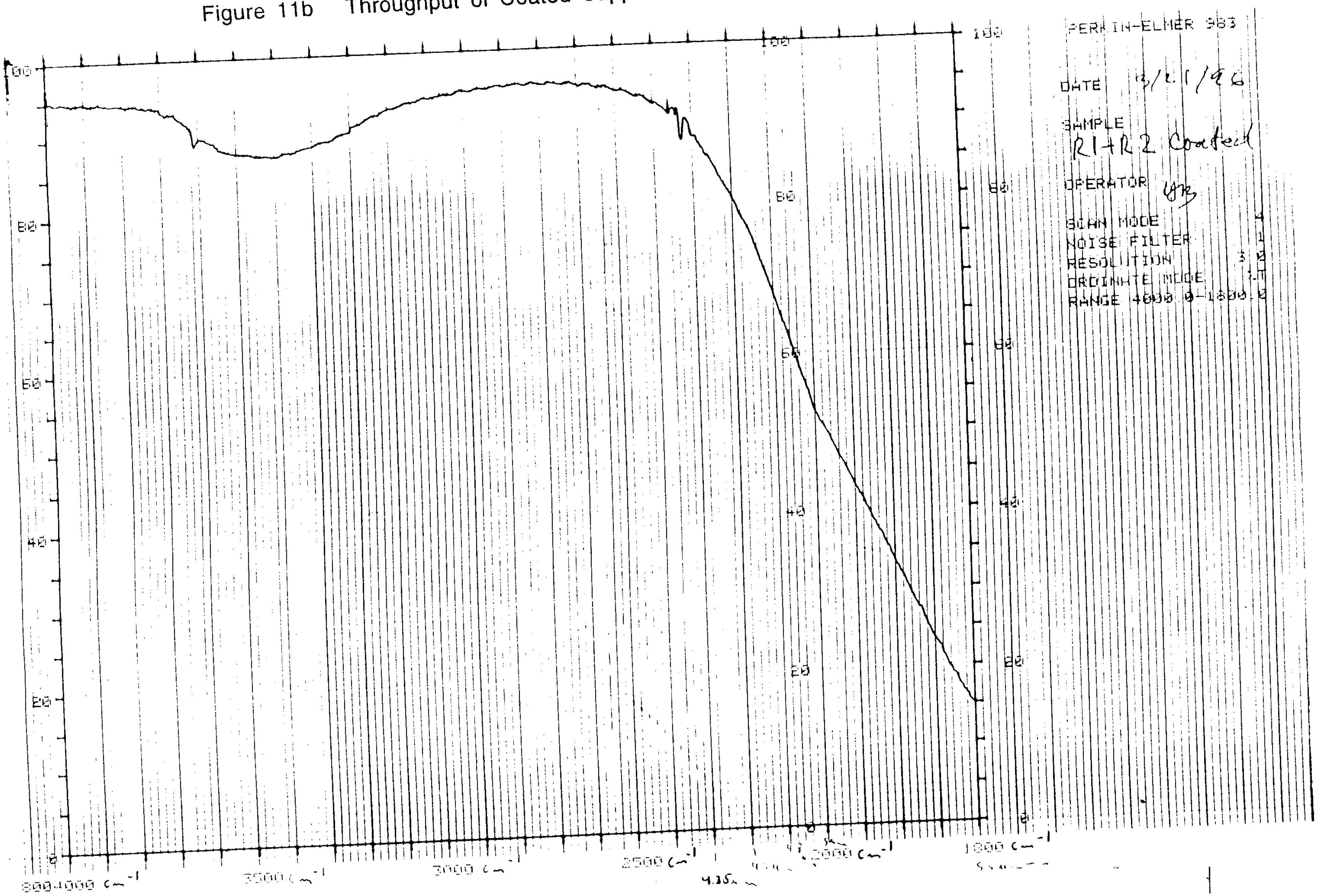

Figure 12 PIDDP Toroidal Slit

HUGHES DANBURY OPTICAL SYSTEMS

HUGHES AIRCRAFT

A432

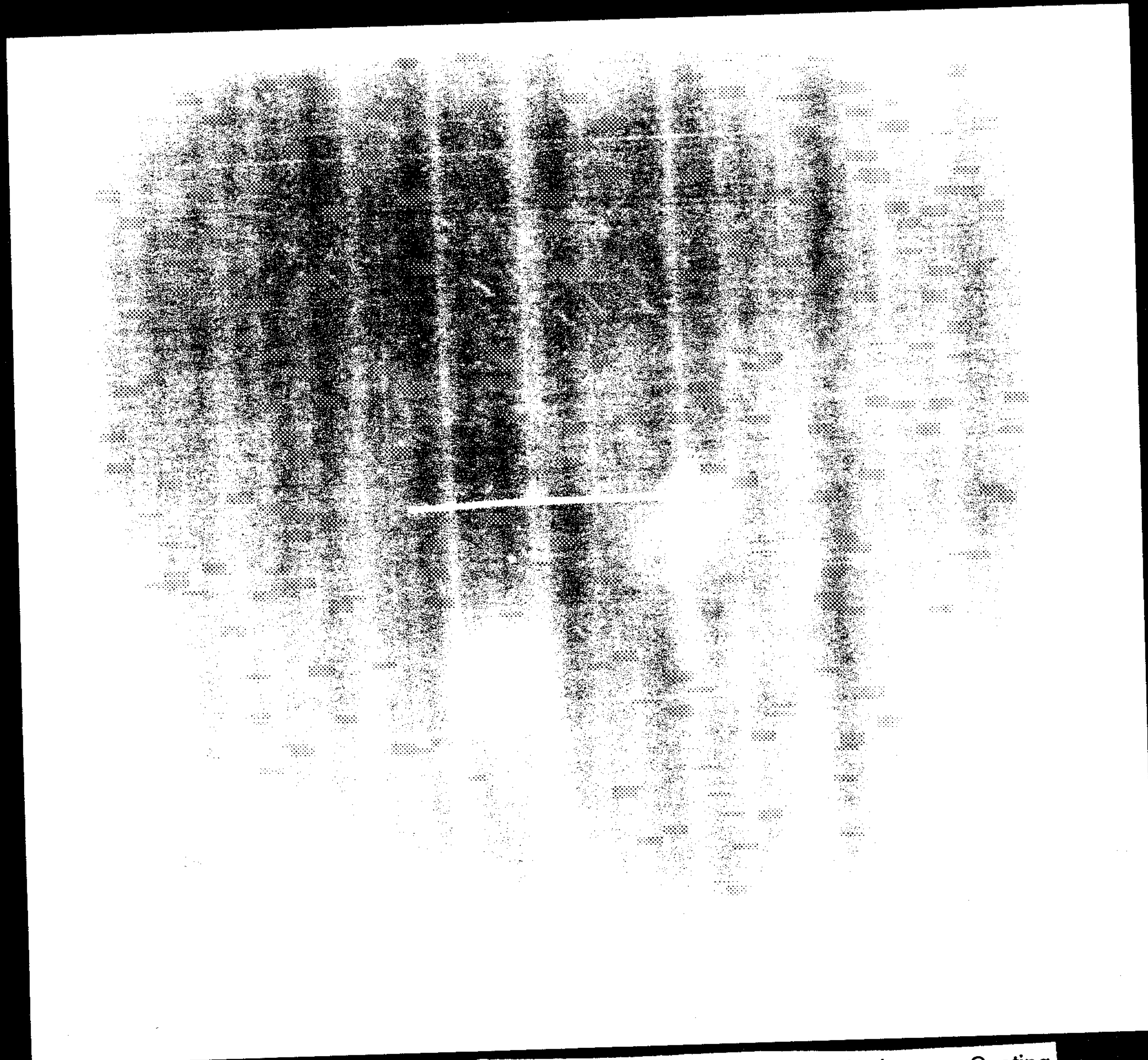

0602-96a

The 40 µm wide slit on the toroidal MgF_2 substrate, coated with chrome. Coating "imperfections" seen are actually reflections from overhead lighting.

Figure 13 **PIDDP Breadboard**

HUGHES DANBURY OPTICAL SYSTEMS HUGHES AIRCRAFT

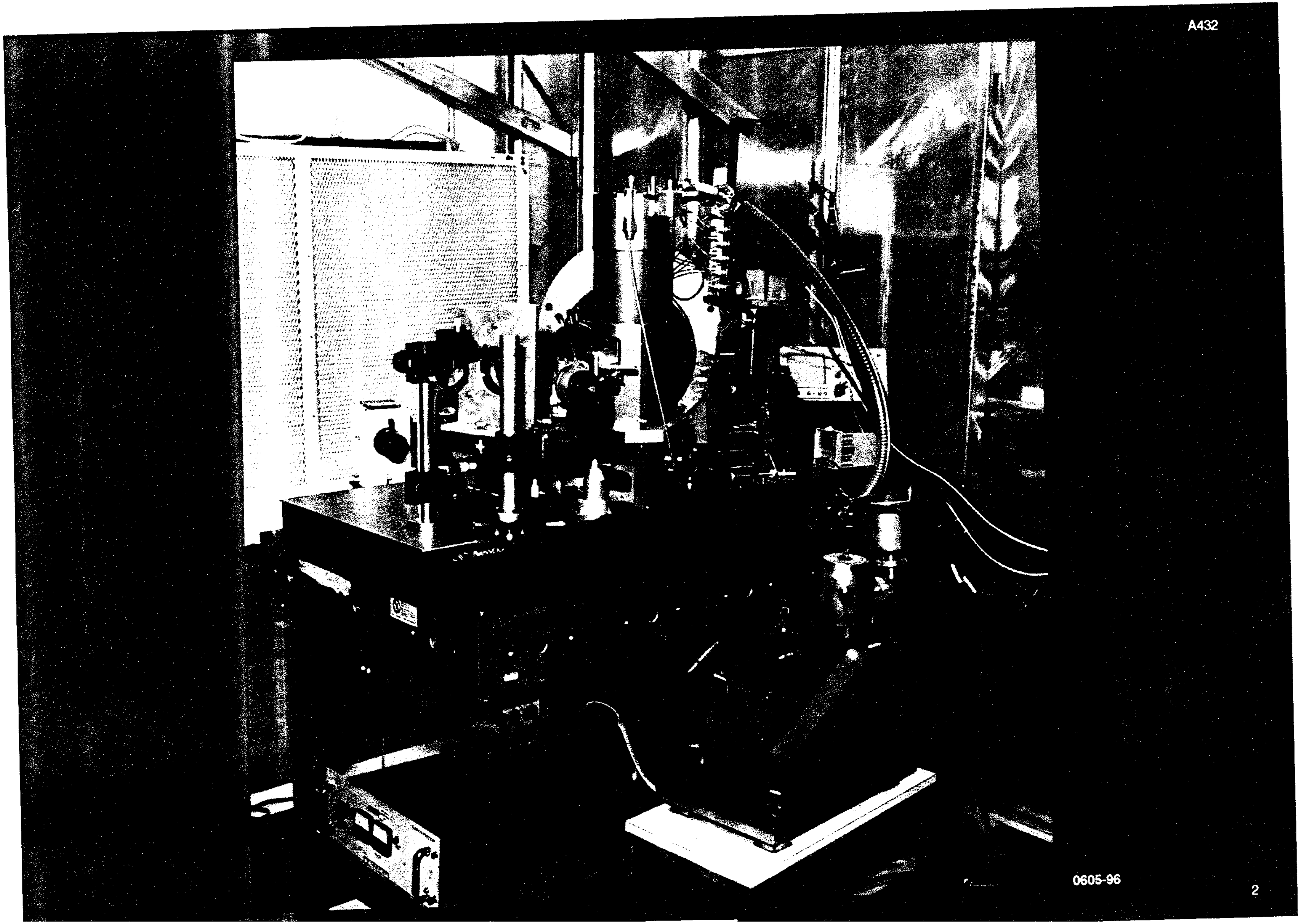

the voltages from the different frames were averaged. A large bias offset was evident in the readout voltages from both integrations. It was felt subtraction of a frame of a short integration time, averaged over a large number of frames to reduce noise, would allow the bias offset to be removed while having minimal effect on the spectrometer background data. Consequently a separate set of a hundred frames each of 10 μseconds duration were taken with the fold flat removed. These voltages were then averaged and the results subtracted from the above background frames. The resulting background voltages from the data are displayed in Figure 14. Note that the three different regions of the HYDICE focal plane are evident in the data. These regions correspond to three different well depths, output amplifier gains, and noise levels. The reduction of background levels when the toroidal slit is utilized is evident. We then ratioed the voltages from the background when the dewar viewed the spectrometer wall to the background from the toroidal slit. Ideally we would expect the gains associated with the three different focal plane regions to cancel, so that a constant reduction factor would be measured across the focal plane. We would expect this ratio to be the ratio of unity (the spectrometer wall should act as part of a blackbody) to the emissivity of the optical train. The expected emissivity of the optical train can be estimated by estimating the emissivity of the prism and each of the five reflections (toroidal slit, fold flat, prism in double pass, spectrometer corrector, spectrometer primary (twice)). We do not have spectral reflectivity measurements for each mirror; however the reflectity of these clean optical surfaces should be between 97% and 99% in the infrared, implying the five optical surfaces should contribute an emissivity between 5% and 15%. The prism, based on its transmission measurements, should have an emissivity of $\approx$ 10% in double pass. Consequently the optical train emissivity should be between 15% and 25%, implying a background reduction ratio between 4 and 7.

While we expected the background reduction ratios for the three different regions to be the same, they were found to be different (Figure 15). For region C the background reduction ratio was found to be 3.8 ± 0.2, for region B it was found to be 6.0 ± 0.3, and for Region A it was found to be 11.2 ± 2.7. These results are consistent with our expected range for background reduction of between 4 and 7. While region A, because of its high noise, is consistent with the results of the other two regions, the background reduction in Region

Figure 14 BACKGROUND DATA
Background with Toroidal Slit in Place (blue), is reduced from
the Background of Spectrometer Wall (red)

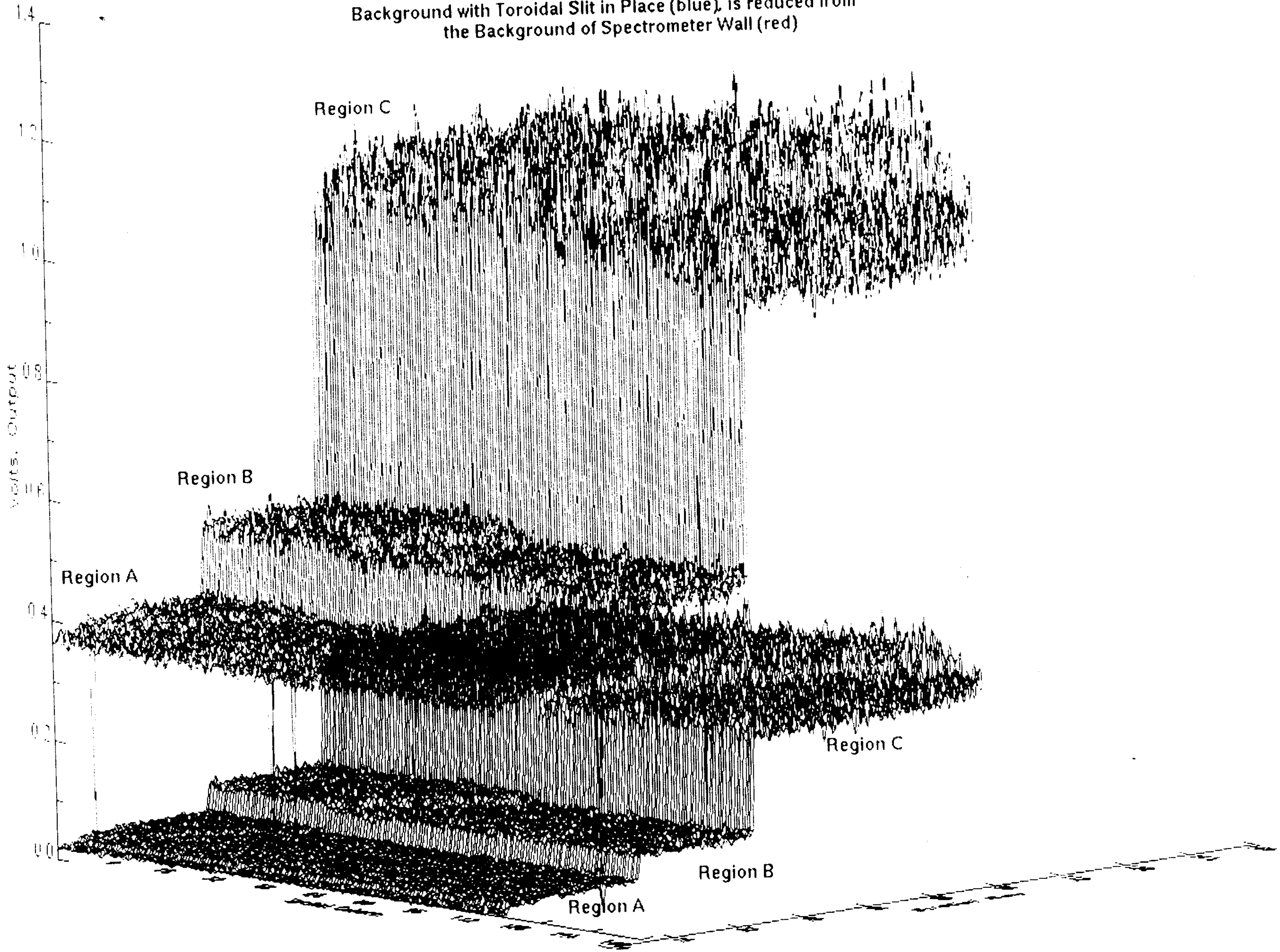

Figure 15 Background Reduction Factors

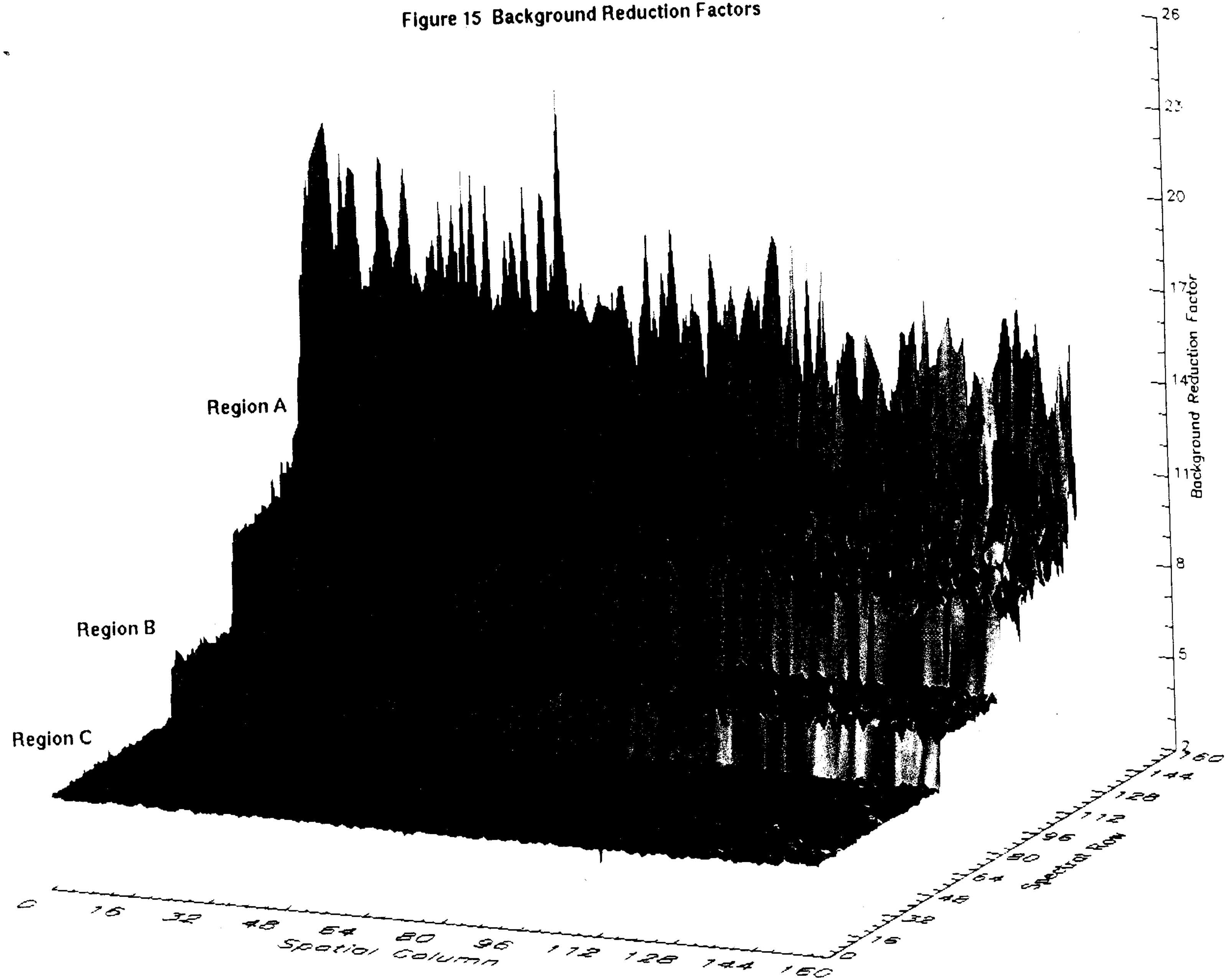

B is significantly different (5.5σ) from that for region C. We do not have an explanation for this significant difference.

In addition to the background reduction provided by the toroidal slit, we expect the cold stop of the reflective relay to also significantly reduce background relative to the original HYDICE configuration. The HYDICE focal plane had a view of the spectrometer cavity of 0.36 sr. For PIDDP this view is reduced to the 0.087 sr view of the f/3 beam. Consequently from the cold stop geometry alone, we should observe $\approx$ 4.1 background reduction in PIDDP relative to a HYDICE viewing a background out to the InSb cut-off. Of course we do not have measurements of a HYDICE design spectrometer working out to the InSb cut-off (HYDICE has a cold filter to restrict the background to 2.5 μm). But we can calculate the background a pixel subtending a 0.36 sr solid angle viewing a 23°C spectrometer to the InSb cut-off would observe in a 60 μsecond integration time. A thermal background integration indicated 2.24 million electrons would be observed. Given measured HYDICE gain factors of 1.1 μV/electron for Region C, of 0.43 μV/electron for Region B, and 0.25 μV/electron for Region A, we would expect to measure 2.46 volts for Region C, 0.95 volts for region B, and 0.57 volts for Region A. We would expect our measurements of the spectrometer wall to be a factor of 4.1 less than these measurements, due to our cold stop. In fact, as Figure 14 indicates, we measured Region C at 1.13 volts, Region B at 0.546 volts, and Region A at 0.409 volts. This is a factor of only 2.2 less for Region C, 1.7 for Region B, and 1.4 for Region A than the background levels we would expect from a HYDICE with no cold stop. It is difficult to say why the cold stop did not perform to our expectations. It is possible that the gain factors for this HYDICE focal plane reject are substantially different from those of the original HYDICE focal plane. It seems unlikely that there could be sneak paths to the focal plane around the cold stop that would increase the measured background, although further testing would be required to rule it out. It is also possible the invar assembly within the dewar is not well coupled in a thermally conductive manner to the cold plate. In that case the cold pupil would not get cryogenically cold. A temperature of -50°C (rather than the < -170°C expected) would explain the observed difference. Measurements with added thermistors would be required to rule this possibility out.

The total background reduction achieved with the PIDDP breadboard is the product of the measured reductions with the toroidal slit and the calculated reduction from the cold stop. This is (3.8*2.2) = 8.4

for Region C, (1.7*6) =10.2 for Region B, and (1.4*11.2)=15.7 for Region A. Thus the combination of toroidal slit and cold stop indicate background levels a factor of 8 to 10 less than what we believe a comparable HYDICE design would have produced. While we had hoped for a factor of 20 reduction in background from the PIDDP design (original PIDDP proposal, page 7), a factor of 8 reduction would be sufficient for many applications.

A spectrum of a polystyrene was taken by inserting a polystyrene filter in front of the toroidal slit and shining an incandescent lamp through the spectrometer. A series of a hyndred frames, each of 10 μsecond integration were taken and averaged. A set of a hundred frames each of 10 μseconds duration were taken with the polystyrene filter removed. This continuum was then averaged and the results subtracted from the polystyrene spectrum frames' average. Each spectral row, consisting of 160 spatial columns, was then averaged. This produced an absorption spectrum for the polystyrene. The standard spectrum for polystyrene is displayed in Figure 16; the spectrum taken by the PIDDP spectrometer is shown in Figure 17. Gain corrections have been applied to the three different focal plane spectral regions to generate this spectrum. Note that the spectrum falls off in intensity after 4200 nm due to the decrease in the spahire prism transmission (Figure 11b). Because the PIDDP breadboard spectrometer has an average spectral resolution of 22 nm the spectrum of Figure 17 is smoothed out relative to that of Figure 16. Note that the spectrum taken with the PIDDP breadboard spans 450 nm to 4950 nm, the ultraviolet to the infrared, 3.4 spectral octaves. (HYDICE covered < 2.5 spectral octaves).

6.0 CONCLUSIONS

All the objectives of the PIDDP breadboard were achieved. Substantial thermal background reduction relative to the HYDICE hyperspectral imager design was successfully demonstrated. Successful spectrometer operation from the ultraviolet to the infrared was demonstrated.

Figure 16 Polystyrene Standard Spectrum, Taken on a Perkin-Elmer Grating Spectrometer

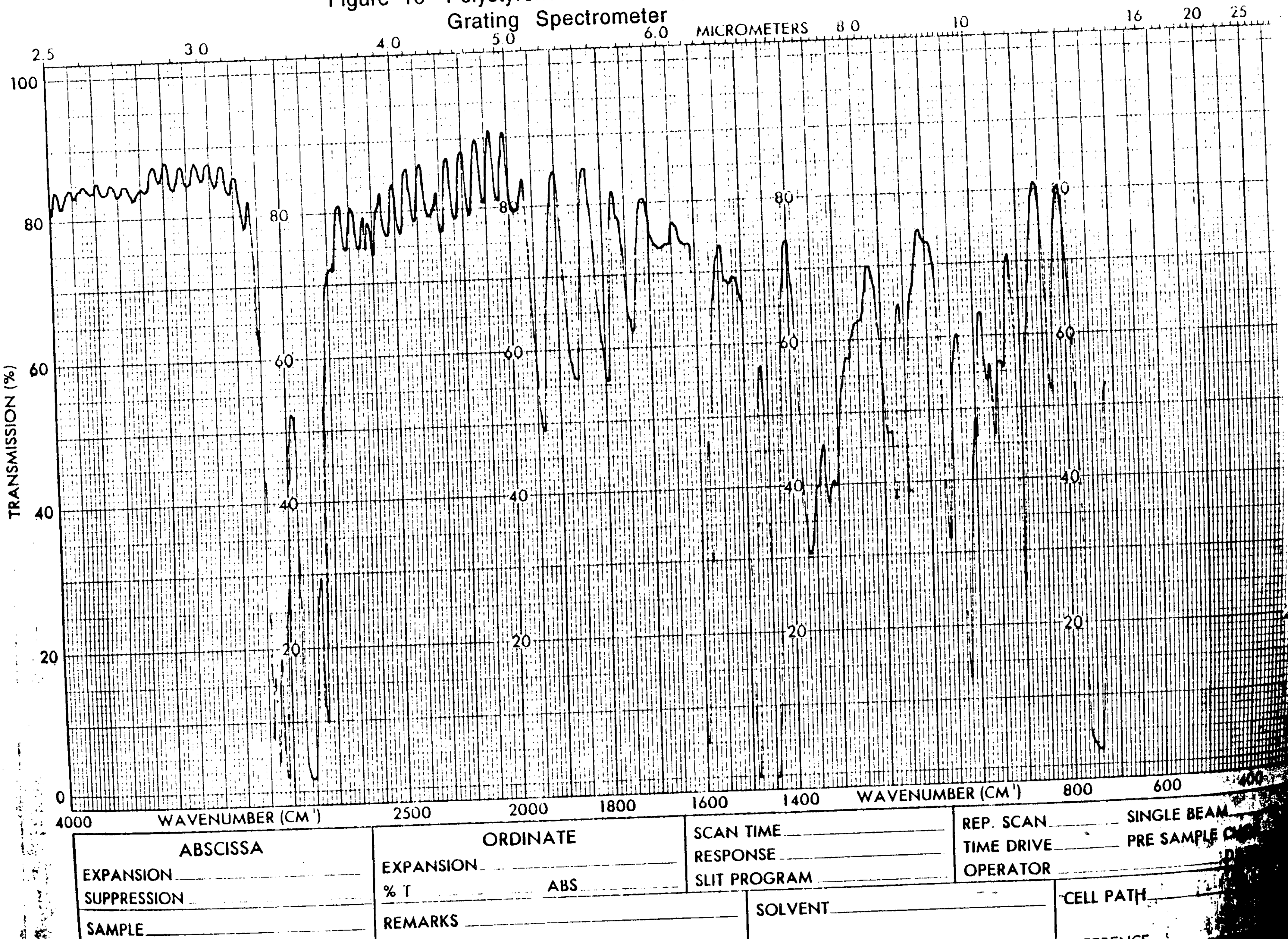

Figure 17 PIDDP Breadboard
Polystyrene Spectrum

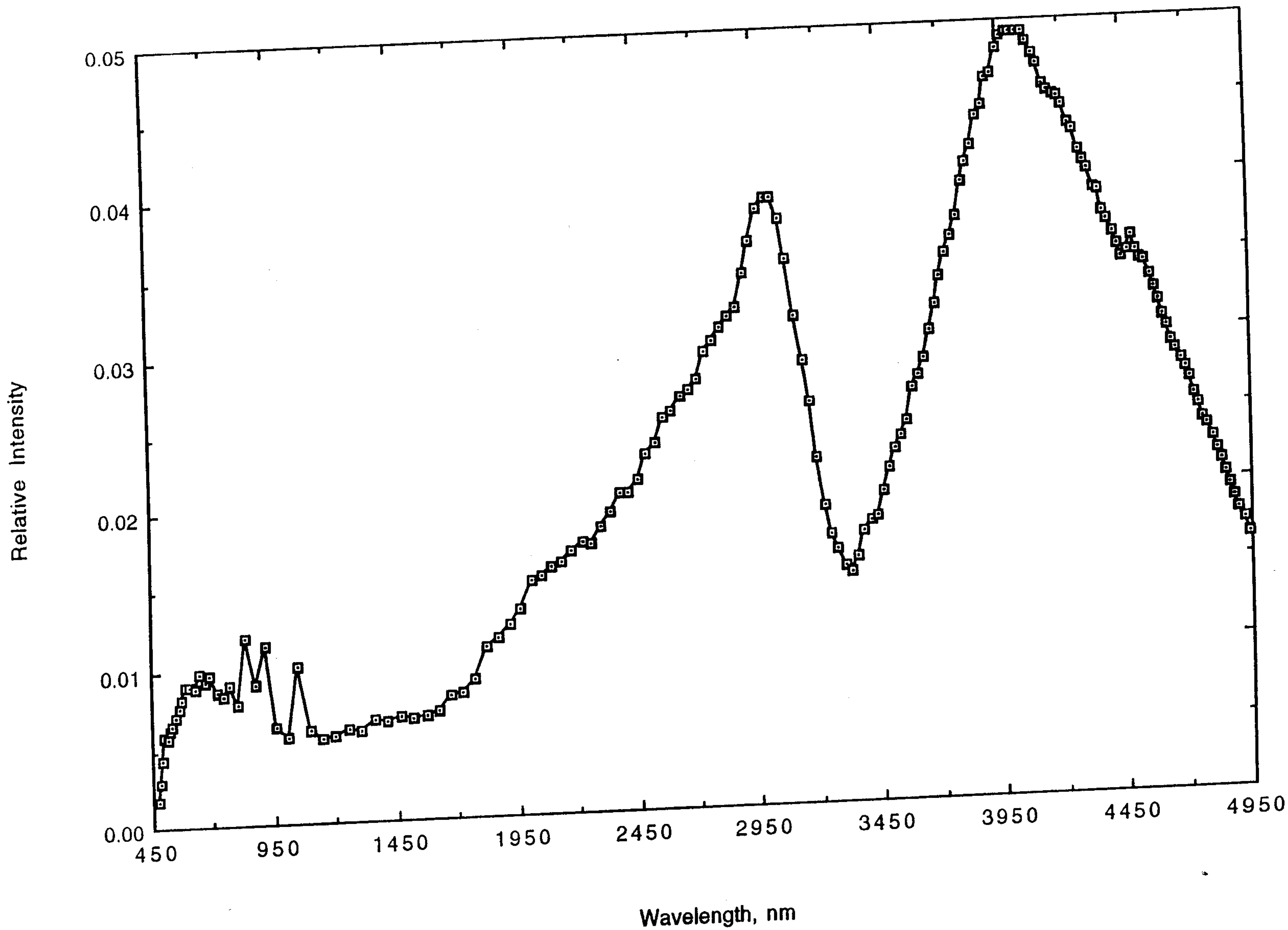

REPORT DOCUMENTATION PAGE

Form Approved
OMB No. 0704-0188

1. AGENCY USE ONLY (Leave blank)	2. REPORT DATE	3. REPORT TYPE AND DATES COVERED
	11 July 1996	

4. TITLE AND SUBTITLE

Planetary Hyperspectral Imager Breadboard

5. FUNDING NUMBERS

C: NASW-5015

6. AUTHOR(S)

Dr. Peter Silverglate

7. PERFORMING ORGANIZATION NAME(S) AND ADDRESS(ES)

Hughes Danbury Optical Systems, Inc.
100 Wooster Heights Road
Danbury, CT 06810

8. PERFORMING ORGANIZATION REPORT NUMBER

PR C19-0005

9. SPONSORING/MONITORING AGENCY NAME(S) AND ADDRESS(ES)

NASA Headquarters
Acquisition Division
Code HWC Washington, DC 20546-0001

10. SPONSORING/MONITORING AGENCY REPORT NUMBER

11. SUPPLEMENTARY NOTES

12a. DISTRIBUTION/AVAILABILITY STATEMENT

12b. DISTRIBUTION CODE

13. ABSTRACT (Maximum 200 words)

A hyperspectral imaging spectrometer was breadboarded. Key innovations were use of sapphire prism and single InSb focal plane to cover the entire spectral range, and a novel slit optic and relay optics to reduce thermal background. Operation over a spectral range of 450 - 4950 nm ($\approx$ 3.5 spectral octaves) was demonstrated. Thermal background reduction by a factor of 8 - 10 was also demonstrated.

14. SUBJECT TERMS

Hyperspectral; Spectroscopy; Thermal Infrared Background Spectrometer

15. NUMBER OF PAGES

16. PRICE CODE

17. SECURITY CLASSIFICATION OF REPORT	18. SECURITY CLASSIFICATION OF THIS PAGE	19. SECURITY CLASSIFICATION OF ABSTRACT	20. LIMITATION OF ABSTRACT
Unclassified	Unclassified	Unclassified	UL

NSN 7540-01-280-5500

Standard Form 298 (Rev. 2-89)
Prescribed by ANSI Std. Z39-18
298-102